Journal of Powder & Bulk Solids Technology 3 (1979) 4; 15–21

A PROPOSAL OF A NEW CHARACTERIZATION OF PARTICLE SHAPE AND ITS APPLICATION

J. Tsubaki and G. Jimbo
Department of Chemical Engineering
Nagoya University,
Furo-cho, Chikusa-ku, Nagoya, Japan 464

Particle shape characterization has long been considered in terms of various factors and indices but these have been of little practical benefit in the past. The advent of modern electronic techniques and the development of computers facilitate more sophisticated numerical analysis of images. This paper proposes a novel series of shape indices, based on classical concepts, and discusses their relationship. These indices may be correlated mathematically and also displayed on triangular diagrams so as to give clear indications of particle morphology, showing particularly the influence of elongation and convexity or concavity. This work makes possible the identification of particles according to their shape characteristics.

INTRODUCTION

Two kinds of shape factors have been widely used in Powder Technology, one being the shape coefficient and the other being the shape index. The former is determined as the coefficient that characterizes the effect of particle shape in the equations that describe the physical properties or behaviour of powders. Volume and surface shape factors are typical examples. The second is, on the other hand, to express the shape itself morphologically and mathematically, independent of physical phenomena. Sphericity and elongation are typical examples.

Though various kinds of shape factors have been previously proposed, few of them had practical applicability for the analysis of real powder particles until the recent development of electronic techniques and the application of computers to make more detailed numerical analysis of images possible. This means that the shape index has come to be available for more numerical treatment and to more practical applications.

The shape indices obtained by such advanced techniques also open a new way to the statistical analysis of powder shape which has only scarcely been studied and reported until quite recently.

In this report, some new shape indices are defined as the ratios of various kinds of characteristic diameters, and are represented in triangular coordinates specifically proposed herein. For evaluation, each index is compared on the triangular coordinate chart. The distribution of the shape indices proposed here are also investigated by analysing both model shaped figures and the images of real particles.

The results show that these shape indices will be sufficiently applicable to shape analysis, as follows.

NOMENCLATURE

d_A	arithmetic mean diameter of breadth and length
d_F	Feret's diameter
d_H	Heywood's diameter (projected area diameter)
d_L	diameter of the circle of equal perimeter
d_R	diameter of unrolled perimeter
$E(d_F)$	expectation of Feret's diameter
$E(d_R)$	expectation of diameter of unrolled perimeter
F	cumulative frequency
G	centre of gravity of projected figures
P	digitized point on the perimeter of a particle
R	radius (distance between P and G)
Z	elongation
Z'	transformed elongation
θ	orientation of a particle
ψ	shape characteristic defined as the ratio of mean diameters
ψ_{max}	maximum value of ψ
ψ'	transformed ψ
ψ_{FL}	d_F/d_L
ψ_{HA}	d_H/d_A
ψ_{HF}	d_H/d_F
ψ_{HL}	d_H/d_L (circularity)
ψ_{RH}	d_R/d_H
ψ_{RL}	d_R/d_L

DEFINITIONS OF SHAPE INDICES

All shape indices, except for elongation Z, can be defined as the ratios of characteristic diameters. Characteristic diameters used in this report are as follows:

d_H diameter of the circle with equal area (Heywood's diameter)

d_L diameter of the circel with equal perimeter,

d_A diameter of the arithmetic average of breadth and length

d_F Feret's diameter

$E(d_F)$ the expectation of Feret's diameter

$E(d_R)$ the expectation of unrolled diameter d_R

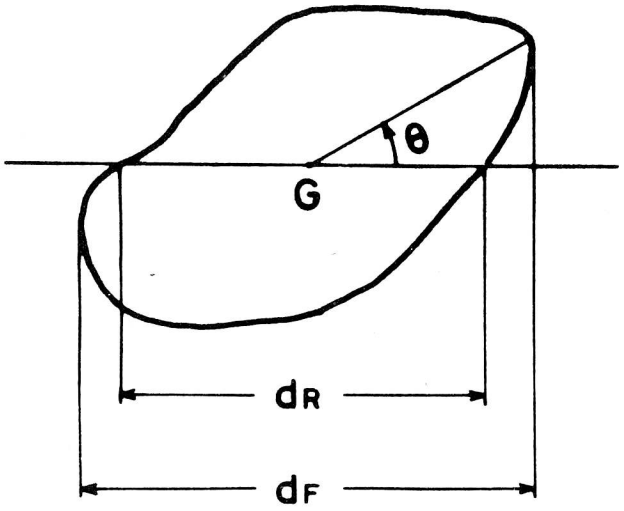

Figure 1. Definition of Feret's diameter d_R and unrolled diameter d_F.

The unrolled diameter d_R is determined by the chord length through the centre of gravity as shown in **figure 1**. Also, the expectation of d_R can be obtained as twice the expectation of radius R, which can, in turn, be obtained as the distance between the centre of gravity and a point on the perimeter unrolled around its centre of gravity. As both Feret's diameter, d_F, and unrolled diameter, d_R, depend upon the particle orientation θ their expectations may be expressed by the following equations:

$$E(d_F) = \frac{1}{\pi}\int_0^{\pi} d_F d\theta \qquad (1)$$

$$E(d_R) = \frac{1}{\pi}\int_0^{\pi} d_R d\theta = \frac{1}{\pi}\int_0^{2\pi} R d\theta \qquad (2)$$

Applying these mean diameters, six shape indices may be defined as in equations (3) to (8):

$$\psi_{HL} = d_H/d_L \qquad (3)$$

$$\psi_{RH} = E(d_R)/d_H \qquad (4)$$

$$\psi_{RL} = E(d_R)/d_L \qquad (5)$$

$$\psi_{HF} = d_H/d_F \qquad (6)$$

$$\psi_{FL} = E(d_F)/d_L \qquad (7)$$

$$\psi_{HA} = d_H/d_A \qquad (8)$$

In addition to these indices, elongation Z is also used as a shape index.

Each of the seven indices proposed herein represents a different characteristic of the particle shape, as follows:

ψ_{FL} according to Caucy's theorem, if a particle has no concavity, d_L is equal to $E(d_F)$ and, therefore, the index ψ_{FL}, being their ratio, can clearly indicate the existence of concavity. ψ_{FL} is unity for a circle, a rectangle, and other shapes with no concavity.

ψ_{RH} as the authors have previously indicated[1], $1/\psi_{RH}$ increases linearly with any increase in the deviation of unrolled diameter reduced by its expectation. It is expected that ψ_{RH} indicates the degree of elongation of shape rather than particle concavity or convexity.

ψ_{RL} it was also shown in a previous report[1] that ψ_{RL} is related to a function of $dR/d\theta$, if the points on the perimeter are described by $R-\theta$ axis. It is, therefore, expected that ψ_{RL} will be a good indicator of particle concavity and convexity. ψ_{RL} is unity only for a circle.

ψ_{HF} this is the circularity of a figure found by tangent lines of the image of the particle to be analysed, but tangents with intersections on the perimeter must be eliminated and, therefore, the tangent with two points of contact on the perimeter of the original figure at a concavity, formed a part of the perimeter of this modified figure. Therefore, if an original figure has no concavity, ψ_{HF} has the same value as ψ_{HL}. It is only equal to unity for a circle.

ψ_{HA} all the previously defined shape factors have a maximum value of unity except for ψ_{HA} which has a maximum value of 1.13 for a square.

As is evident from the definition of shape index, one shape index may be considered as the product or quotient of the other indices, as shown in equations (9) and (10):

$$\psi_{RL} = \psi_{RH} \cdot \psi_{HL} \qquad (9)$$

$$\psi_{HL} = \psi_{HF} \cdot \psi_{FL} \qquad (10)$$

From these relationships, it is expected that two kinds of triangular diagram approaches may be proposed to compare particle shapes. We term these as the RHL diagram and the FHL diagram according to the factors considered, as are illustrated in equations (9) and (10). Both triangular diagrams are illustrated in **figures 5–8 and 9–11**.

SAMPLES USED AND EXPERIMENTAL PROCEDURE

Three kinds of sample material were selected to check the newly defined indices. These were limestone **(figure 2)** as a crystalline material, crushed glass **(figure 3)** as an amor-

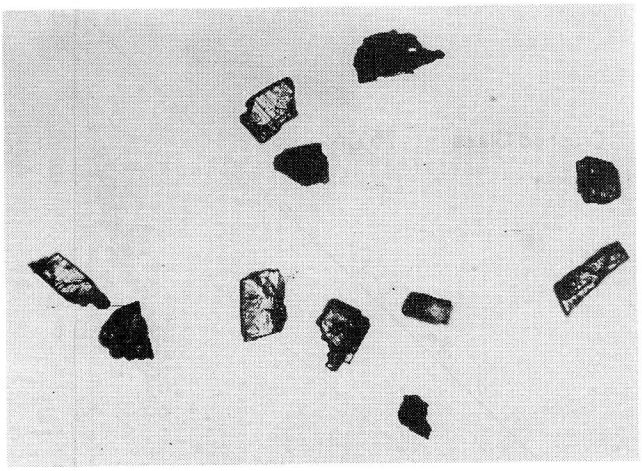

Figure 2. Limestones classified hydrodynamically (the average diameter is 75 μm in settling velocity diameter).

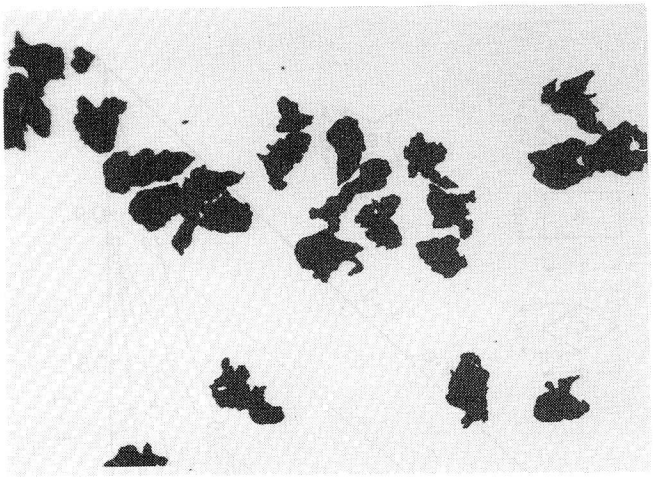

Figure 4. Atomized stainless steel powder classified hydrodynamically (the average diameter is 135 μm in settling velocity diameter).

phous material, and atomized stainless steel powder (**figure 4**) as a markedly concave-shaped particle.

Two kinds of limestone and crushed glass were prepared of average particle size 550 μm and 75 μm. Only one size of 135 μm was used for the stainless steel samples. As these samples were hydrodynamically classified, their average diameters were expressed in terms of free-falling diameter. The number of sample particles examined were 214, 203, 244, 98 and 129 for larger and smaller limestone and crushed glass particles and atomized stainless steel particles respectively.

The images of the particles were fixed photographically by microscope and each particle was analysed with the stylus-pen (graf-pen) digitizer.

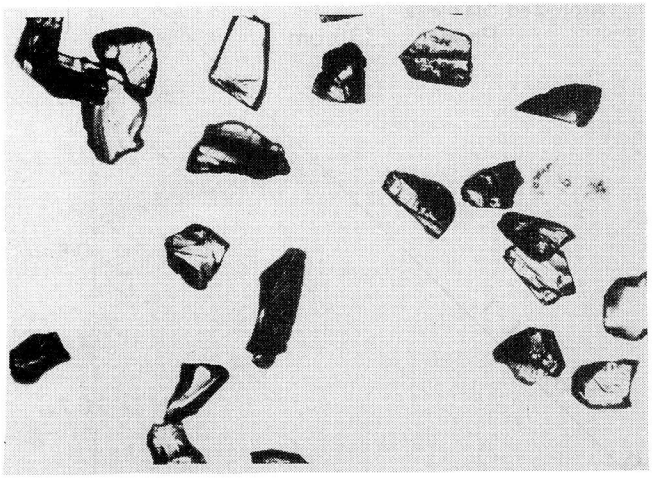

Figure 3. Crushed glasses classified hydrodynamically (the average diameter is 75 μm in settling velocity diameter).

RESULTS AND DISCUSSION

Values of shape indices obtained were plotted on the previously described triangular diagrams and are shown in **figures 5–8.** They were also plotted on a log-normal chart to represent the distribution of sample shape index, as shown in **figures 9–11.** It is possible, with these diagrammatic shape representations to perform a morphological identification of the particles, as follows:

Triangular Coordinates Method

RHL Diagram: The shape indices of geometrically modelled shape, shown in **figure 5.** It shows that the value of ψ_{RH} varies with elongation rather than concavity or convexity. The value of ψ_{RL}, however, depends mainly on concavity or convexity.

The results for real samples are shown in **figures 6–8.** It is quite clear that the data for atomized stainless steel powders are scattered on the RHL diagram but, in contrast, those for crushed glass and limestone are relatively concentrated. It may suggest that the shapes of crushed glass and limestone vary in similar manner. As the data for atomized stainless steel powders distribution is close to the ψ_{RL} axis, it can be estimated that such powders have some concavity or convexity. Though the results are not shown here, the data for larger particles distributes itself in the upper region of the RHL diagram indicating a simpler shape than for the smaller particles.

FHL Diagram: As already pointed out, this diagram can reveal the existence of particle concavity since $\psi_{FL} = 1$ only if there is no concavity. The results, shown in **figures 9–11** indicate that the data for limestone lies principally in the upper region, below it crushed glass and then the atomized stainless steel. The latter is closer to the central portion of the diagram. This order corresponds well to the figures for real particles shown in **figures 9–11.** These figures show that atomized stainless steel powders have more appreciable concavities and convexities and that the decrease is in order of limestone then crushed glass.

In the case of limestone and crushed glass, ψ_{FL} is constant in spite of the variations in ψ_{HL} and ψ_{HF}, but in the case of the atomized powders ψ_{FL} increases with increase in ψ_{HL} and ψ_{HF}. This indicates that in the case of limestone and crushed glass, the traditional circularity ψ_{HL} does not vary with concavity or convexity but with elongation. With the atomized powders, however, ψ_{HL} does vary with concavity and convexity.

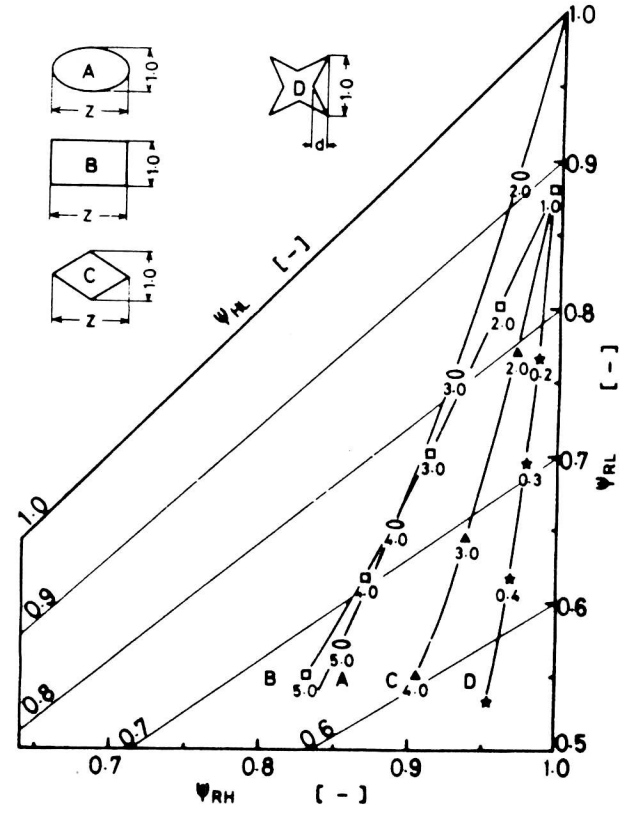

Figure 5. RHL diagram of model shape.

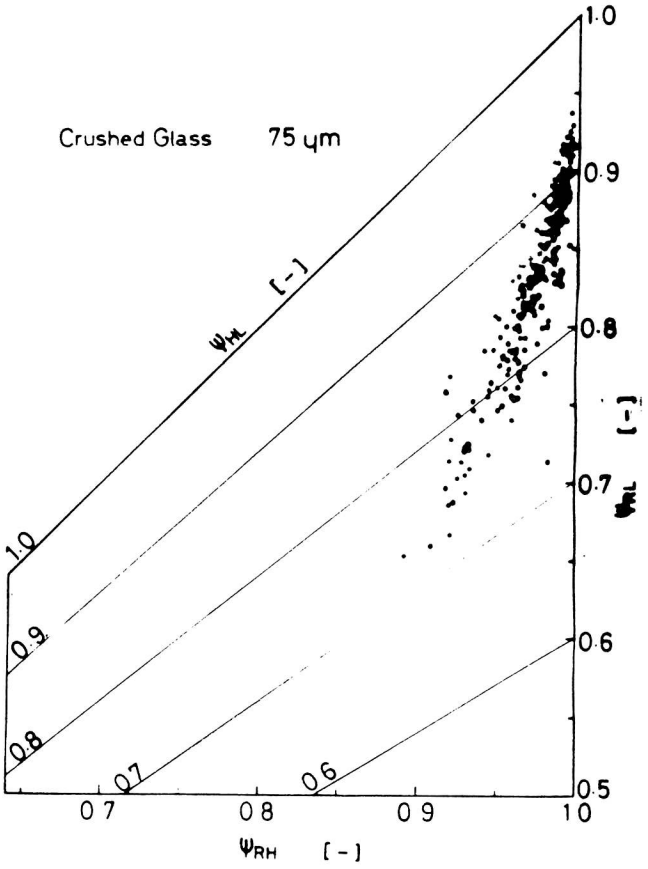

Figure 7. RHL diagram of 75 μm crushed glasses.

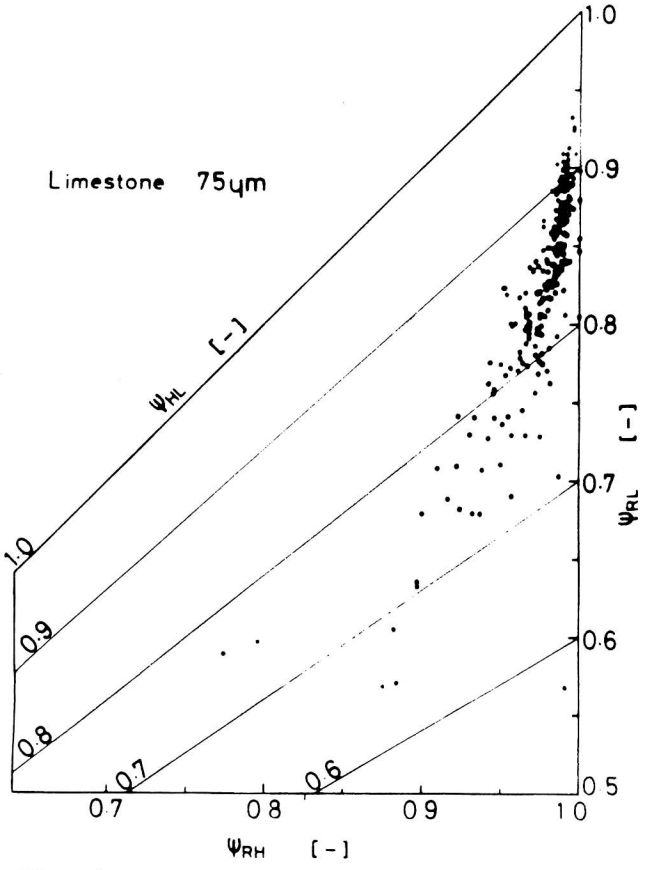

Figure 6. RHL diagram of 75 μm limestones.

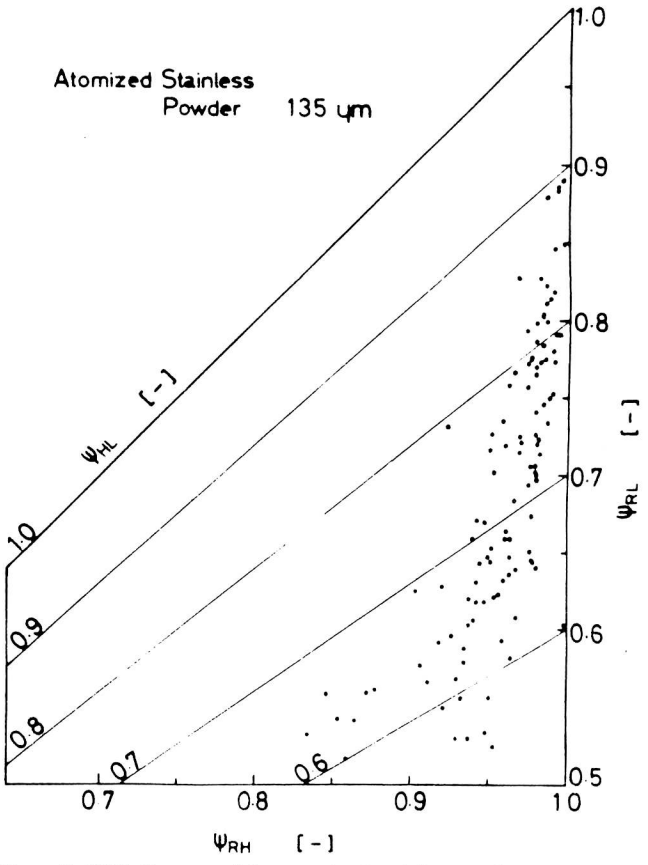

Figure 8. RHL diagram of the atomized stainless steel powder.

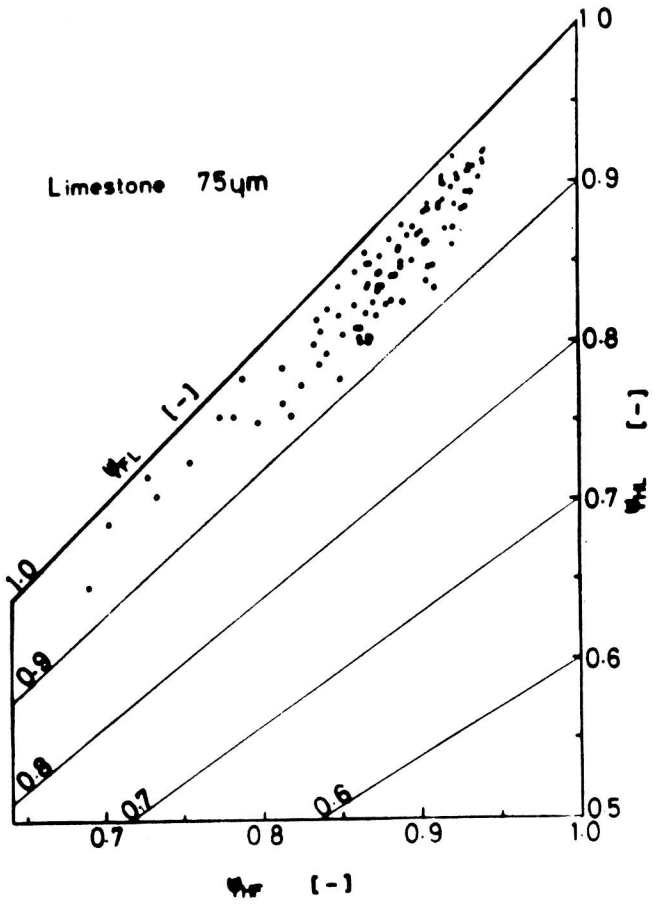

Figure 9. FHL diagram of 75 μm limestones.

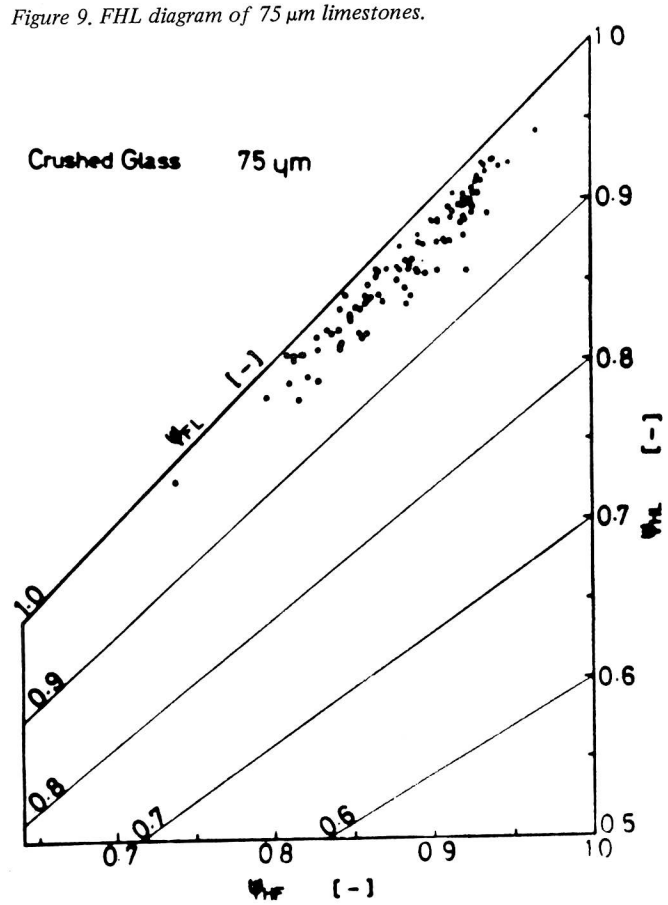

Figure 10. FHL diagram of 75 μm crushed glasses.

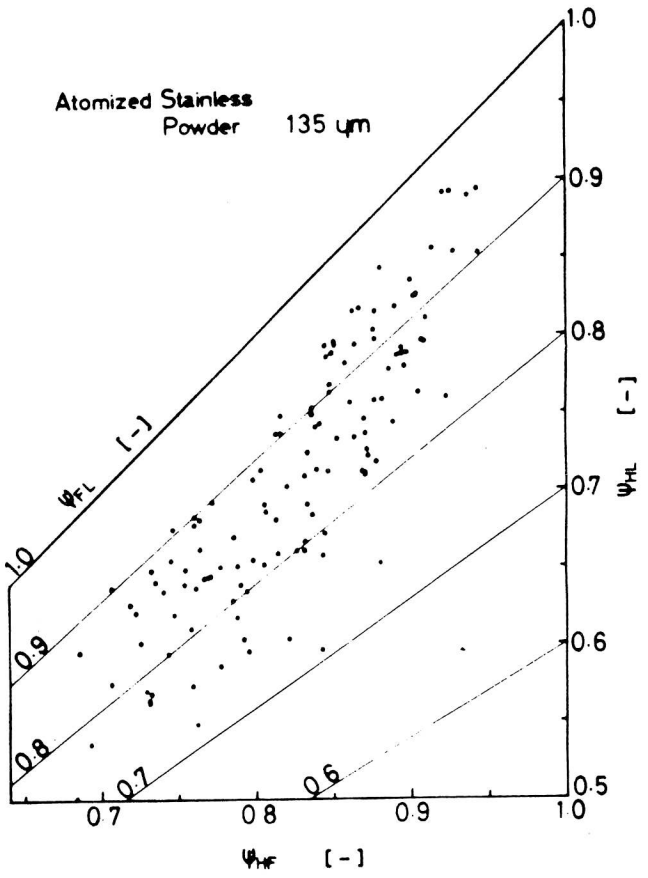

Figure 11. FHL diagram of the atomized stainless powder.

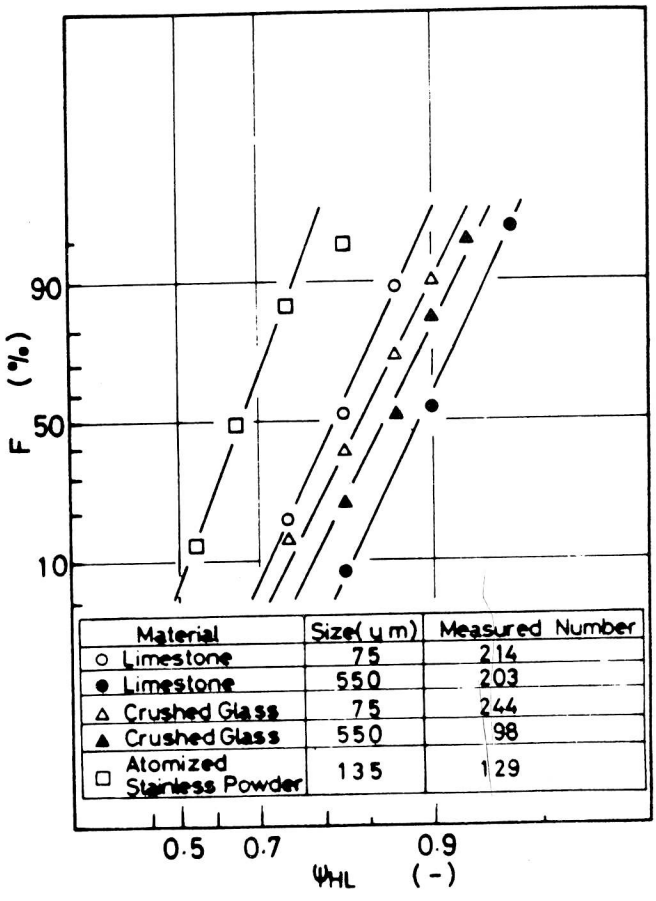

Figure 12. Cumulative frequency of ψ_{HL}.

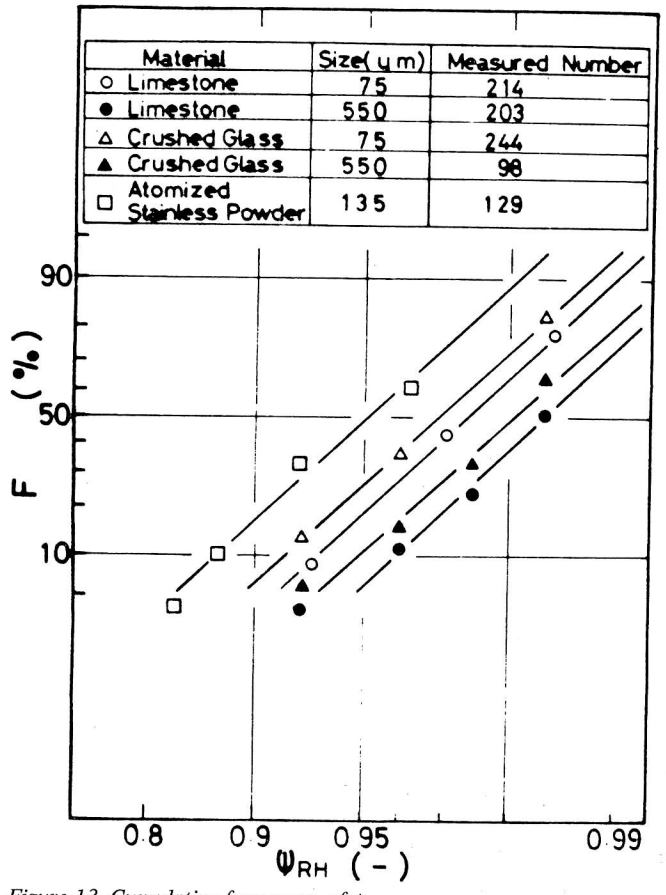

Figure 13. Cumulative frequency of ψ_{RH}.

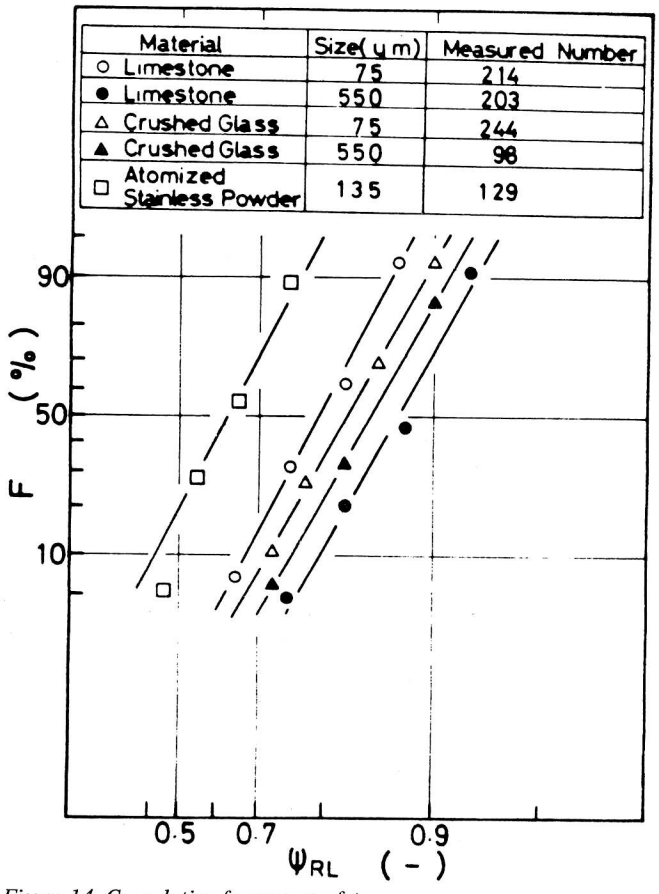

Figure 14. Cumulative frequency of ψ_{RL}.

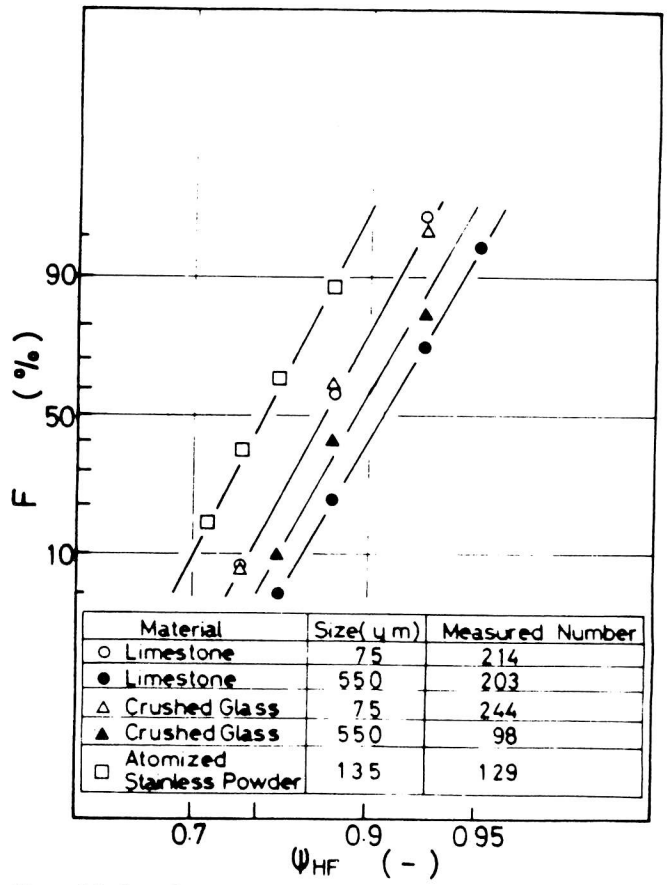

Figure 15. Cumulative frequency of ψ_{HF}.

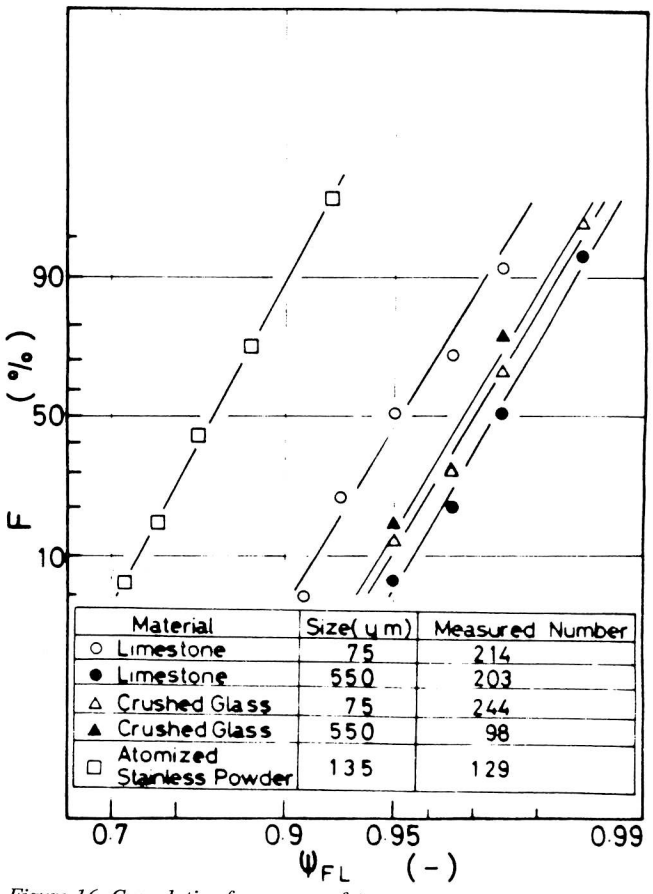

Figure 16. Cumulative frequency of ψ_{FL}.

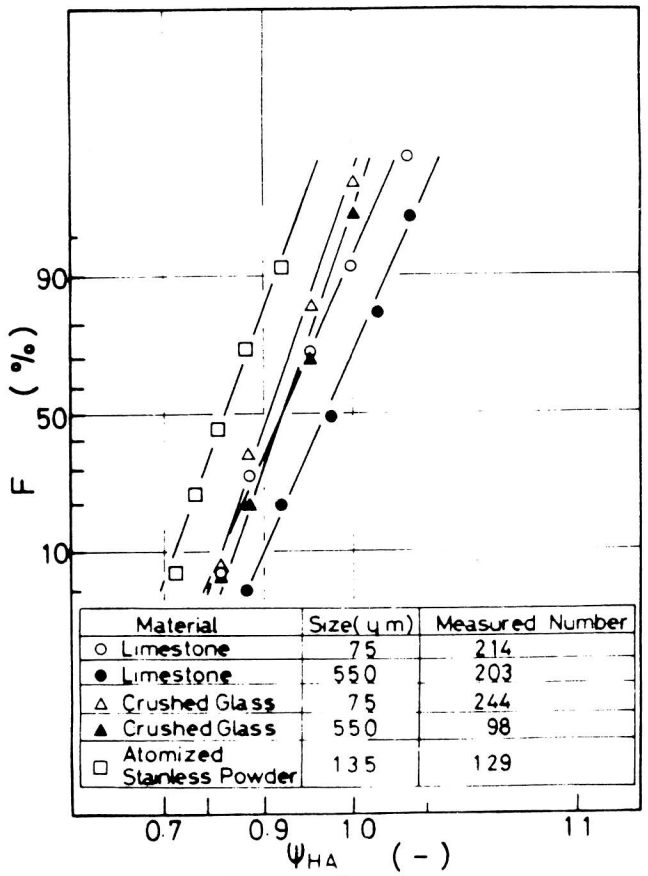

Figure 17. Cumulative frequency of ψ_{HA}.

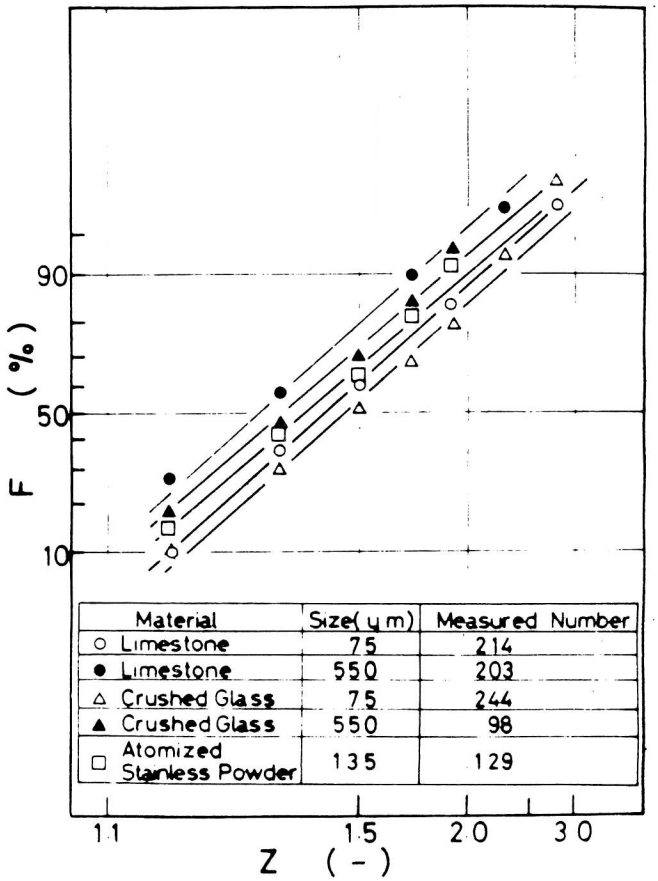

Figure 18. Cumulative frequency of Z.

Distribution Function of Shape Characteristics

The distribution of each shape index for a real powder is shown in **figures 12–18.** These figures suggest that the shape indices, or the modified shape indices defined below, can be satisfactorily represented by a log-normal distribution. But the shape indices ψ determined as the ratios of mean diameters must be transformed to ψ' using equation (11), and elongation Z to Z′ using equation (12):

$$\psi' = \psi_{max} - \psi \tag{11}$$

$$Z' = Z - 1 \tag{12}$$

Considering the indices ψ_{HL}, ψ_{RH}, ψ_{RL}, ψ_{HF} and ψ_{FL}, the maximum value, ψ_{max}, is unity, being equivalent to the case of a circle, but ψ_{HA} has ψ_{max} equal to 1.13 being equivalent to a square. For all these shape indices, except ψ_{HL}, for the crushed glass, the geometric standard deviations of each shape characteristic depends on neither material nor particle size, but the geometric mean does vary with material and particle size. In the case of ψ_{HA} for crushed glass, the geometric standard deviations are also independent of particle size. As the effect of material on shape characteristics is greater for ψ_{FL} and lesser for Z, it is not elongation but rather concavity and convexity that characterizes the particles. The atomized stainless steel samples are especially distinguished from the other samples by ψ_{FL}. Shape indices for the larger limestone particles approach the values for a circle when compared with those for smaller limestone particles. This suggests that both elongation and concavity/convexity for limestone are greater as the particle size decreases. For crushed glass, there is an appreciable dependence of ψ_{RH} and Z on the particle size, but ψ_{RL} and ψ_{FL} are almost independent of particle size. It is, thus, found that the morphological variation of crushed glass relative to particle size differs markedly from that of limestone. The variations for crushed glass are mainly due to elongation.

CONCLUSIONS

The above results can be summarized as follows:

(i) The shape distributions for real powder particles expressed in terms of the shape indices proposed herein all conform to a log-normal distribution when the indices are slightly transformed.

(ii) The geometric standard deviation of each shape distribution expressed in terms of the proposed shape indices are all constant irrespective of material and particle size, except one. Even in that exceptional case, the geometric standard deviation is constant for the same material, irrespective of particle size.

(iii) Applying the relative relationship of each shape index, particles can be identified according to their shape characteristics. The triangular diagram method is proposed for this purpose.

REFERENCE

1. J. Tsubaki, G. Jimbo & R. Wade, "A study of the shape characteristics of particles", *J. Soc. Materials Sci. Japan,* **24**; 262.